On the Performance Prediction of Optical Transmission Systems in Presence of Filtering

Camille Delezoide, Petros Ramantanis, and Patricia Layec
Nokia Bell Labs Paris-Saclay, Nozay, France
Tel: (+33) 0160408878, e-mail: camille.delezoide@nokia-bell-labs.com

ABSTRACT
We investigate the impact of optical filtering from routing nodes in optical networks, and how to predict it. From measurements in presence of tight optical filtering, we propose a new method relying on an extended back-to-back model for improved prediction of the quality of transmission.
Keywords: fiber optics communications, optical filters, Gaussian-noise model, wavelength routing.

1. INTRODUCTION

Both design and optimization of an optical communication network require accurate models to predict the quality of transmission (QoT) for all demands across the network. In coherent optical communications, the Gaussian-noise (GN) model [1] provides a solid theoretical framework: from a generalized optical signal to noise ratio (OSNR) value accounting for amplified spontaneous emission (ASE) and nonlinear optical noises, a bit error ratio (BER) before forward error correction is determined via the signal to noise ratio (SNR) at decision gate, as defined in [1]. The BER-SNR relation is a well-known, mathematically-derived expression depending on modulation format and coding scheme [2]. In contrast, determining the SNR-OSNR relation typically requires back-to-back calibrations [1] where SNR^{-1} is a linear function of $OSNR^{-1}$ [3,4]. In this context, the typical methods to account for filtering impairments from optical routing nodes come down to a translation of the calibrated SNR_{dB}-$OSNR_{dB}$ curve [5-6].

In this paper, we show these previously reported methods become increasingly inaccurate for stronger filtering. This is a challenge for future optical networks. Indeed, solutions to improve the spectral efficiency of links come with a reduction of guard bands between channels, hence tighter optical filters. Moreover, low-cost coherent solutions for metro networks using wavelength selective switches (WSS) and lasers with relaxed requirements will increase the impact of filtering on QoT [7]. To solve this, we first formulate an extended SNR-OSNR relation to better capture the receiver's behavior in presence of noise and filtering. Through experiments, we assess its validity in presence of tight optical filtering. We then propose a method based on back-to-back calibrations of this extended SNR-OSNR relation to predict the SNR hence the BER for a known filter cascade, and for any OSNR value. We finally compare the accuracies achieved in the prediction of filter penalties between our method and the state of the art, and discuss its applicability to optical transmission networks.

2. EXPERIMENTAL SETUP

The experimental testbed is depicted in Fig.1. An external cavity semiconductor tunable laser (ECL) feeds a polarization PDM-QPSK modulator generating symbols at 32.48 GBd from a 2^{16} pseudo-random binary sequence. The transmitter (Tx) generates an RRC0.01 pulse-shaped signal, first going through a bandwidth-tunable optical filter. Then, the signal goes through the combination of a variable optical attenuator (VOA) and a two-stage erbium doped fiber amplifier (EDFA) working in constant-power mode. Through attenuation settings, various OSNR values are obtained independently of the tunable filter configuration. To achieve the high OSNR values necessary to characterize the SNR-OSNR relation near high SNR limit, we place a fixed 400 GHz-bandwidth optical filter between the two stages of EDFA. On the receiver (Rx) side, we shunt 1% of the signal into an optical spectrum analyzer (OSA) to measure OSNR values for each VOA and tunable filter configuration.

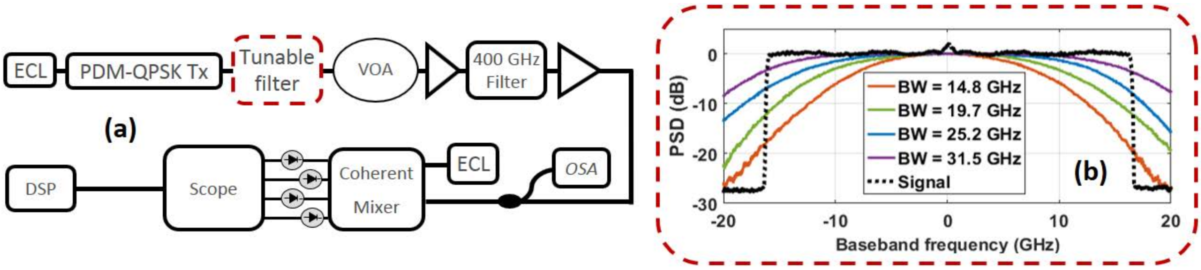

Figure 1: (a) Experimental setup for back-to-back measurements of SNR-OSNR relations and (b) measured optical filter functions for various bandwidth settings and measured signal spectrum at Tx output.

We recover signals using a coherent mixer connected to four 43GHz balanced photodiodes and a second ECL as local oscillator. Photocurrents are sampled at 40GSamples/s by a real-time oscilloscope with 20GHz electrical bandwidth. We store 100µs-long series of samples and process them offline. After skew adjustments and normalization, we perform polarization demultiplexing using a constant-modulus algorithm (CMA) with 25 taps, frequency offset compensation and carrier phase recovery. From final constellation diagrams, we directly measure noise variances and average signal energies from which we deduce the corresponding SNR values as an average over both polarizations. Each recorded point corresponds to an average over five SNR-OSNR measurements.

3. SNR-OSNR RELATION IN PRESENCE OF FILTERING

In digital communications, filtering modifies the temporal shape of the signal which, after sampling, creates inter-symbol interference (ISI). In coherent optical communications, a CMA mitigates ISI simultaneously to polarization demultiplexing. To that aim, CMAs amplify both signal and noise in spectral regions where signal was filtered. For instance, the post-CMA ASE noise variance is given [1] by:

$$\sigma_{ASE}^{2} = \int_{-\infty}^{+\infty} G_{ASE} \cdot \left| H_{Rx}(f) \right|^{2} df \tag{1}$$

where G_{ASE} is the ASE power spectral density (PSD) and H_{Rx} is the transfer function of the receiver including CMA's response. Based on the minimum mean-square error (MMSE) convergence, CMAs are designed to optimize the SNR by balancing ISI mitigation with noise amplification [2]. This means that $\mathrm{H_{Rx}}$ depends on input noise level, thus on OSNR. We thus project the existence of a nonlinear function Φ as $\mathrm{SNR}^{-1} = \Phi(\mathrm{OSNR}^{-1})$ describing the dependence of equalizer's response on input noise. Using Taylor's theorem, we can show that this assertion comes down to writing

$$SNR^{-1} = \sum_{k=0}^{N} \left(R/B \right)^{k} a_{k} OSNR^{-k} \tag{2}$$

where N is the order of the expansion, R the baud rate, B the reference bandwidth for OSNR measurement and $(a_k)_{k=1:N}$ are transponder and filter-dependent parameters. For $N = 1$, Eq.2 simplifies to the SNR-OSNR relation described in [3,4], appearing as an approximation of the general SNR-OSNR relation when filtering is moderate.

In Fig. 2, we apply such SNR-OSNR relations with $N = 1$, 2 and 3 to fit, using a least-square method, the experimental data obtained with various tunable optical filter configurations, corresponding to the various 3 dB-bandwidths achieved. We first observe in Fig. 2(a) that the $\mathrm{SNR_{dB}}$-$\mathrm{OSNR_{dB}}$ curve obtained for the tightest filter ($\mathrm{BW_{3dB}} = 14.8$ GHz) is clearly not a direct translation of the same curve obtained for the widest filter ($\mathrm{BW_{3dB}} = 43$ GHz). The main difference between the two curves appears to be in the slopes of the low-OSNR asymptotes. When $N = 1$, the slope of low-OSNR asymptote is mathematically equal to 1dB/dB. This property, experimentally verified in Fig. 2(a) when filtering is moderate, is not valid anymore for very tight filters. This explains why in Fig. 2(b-c), the mean and maximal fit errors – the differences between experimental and fitted SNR values – rapidly grow when $N = 1$ for a decreasing optical 3 dB-bandwidth. For N =2 and 3, the fit errors are significantly reduced, down to the repeatability of measured SNR/OSNR values, within 0.1 dB.

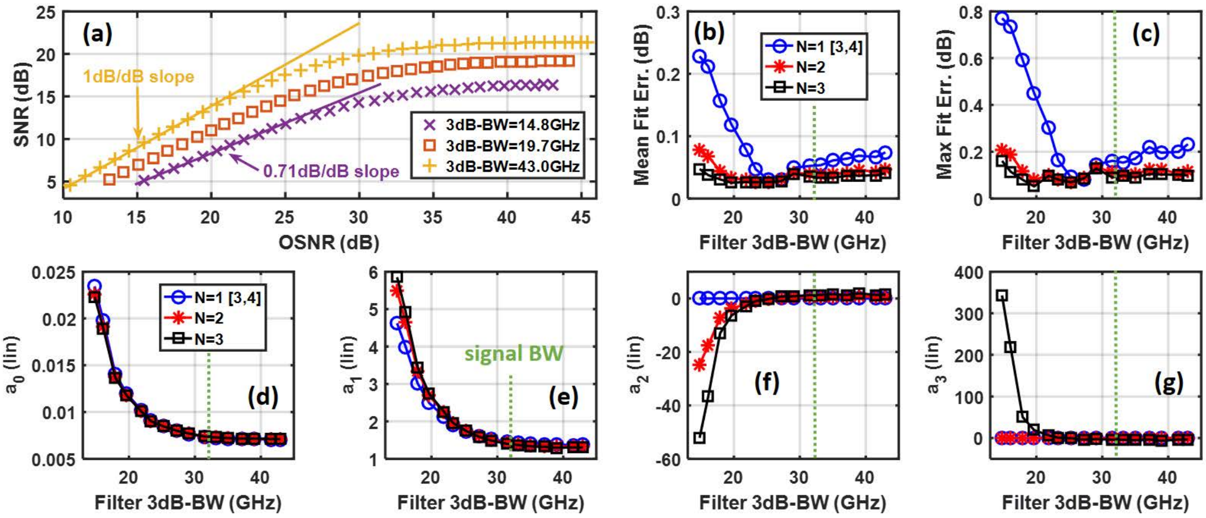

Figure 2: (a) Experimental SNR-OSNR curves for various optical filter bandwidth settings. As functions of the 3 dB-bandwidths tested; (b) Mean fit error; (c) Maximal fit error; and (d-g) Values of fitted a_k parameters.

We notice in Eq. (2) that the zero-order term a_0, independently of the expansion order N, is directly the inverse of the SNR limit when OSNR tends to infinity. In our experiment, since the OSNR is measured before the receiver, we verify SNR = $1/a_0$ when σ^2_{ASE} tends to zero. This means that a_0 represent the noise generated inside the receiver. Evolutions of higher order terms a_k result from CMA amplification of input ASE noise power (cf. Eq. (1)). These coefficients rapidly grow in absolute value when the optical filter bandwidth decreases, as can be observed in Fig. 2(e-g). Indeed, because the equalizer converges towards an optimal SNR, a tighter filter means further dependence of H_{Rx} on the OSNR, hence an exaltation of Φ's nonlinear behaviour characterized by the increase of higher order terms of Eq. (2). Additionally, we observe in Fig. 2(d-g) that a_k values are stable for bandwidths exceeding the baud rate, but rapidly increase – in absolute value – for narrower filters. The use of an RRC pulse shape with 0.01 roll-off explains this behaviour: optical filtering becomes significant when the optical filter 3 dB-bandwidth is shorter than the signal 3dB-bandwidth at transmitter's output, equal to 32.5 GHz (cf. Fig. 1b).

4. APPLICATION TO BER PREDICTIONS

In the following, we assume as typically done in the GN model [1] that SNR_{dB}-$OSNR_{dB}$ curves calibrated in back-to-back, where OSNR only accounts for ASE noise, still apply to optical transmissions where the generalized OSNR accounts for both ASE and nonlinear optical noise. Based on the SNR-OSNR relation proposed in section 3, we derive a five-step method to predict BER in presence of filtering:

(1) Inserting a tunable optical filter in between Tx and Rx as in Fig. 1, we perform back-to-back calibrations to obtain SNR_{dB}-$OSNR_{dB}$ curves for various filter bandwidths.
(2) We fit SNR_{dB}-$OSNR_{dB}$ curves using the extended SNR-OSNR relation (Eq. (2)) to calculate a_k values for various known filter bandwidths. N is adjusted to the worst-case filter.
(3) We characterize the filter cascade by its 3dB-bandwidth denoted BW_{new}, and determine corresponding $a_{k,new}$ values by interpolation of the data gathered during step 2.
(4) We calculate the generalized OSNR value using the GN model [1]. Note that we need to account for insertion losses from cascades filters. Then, inputting $a_{k,new}$ and OSNR values in Eq. (2), we calculate the SNR value.
(5) We convert the SNR into BER using well-known analytical expressions [2].

The tunable optical filter in step 1 can be replaced by an actual filter cascade. Replacing 3dB-bandwidth BW by number M of cascaded filters in steps 1-3, SNR_{dB}-$OSNR_{dB}$ curves can be calibrated for selected M values to predict the BER for an uncalibrated number M_{new} of cascaded filters.

In the following, we test a key aspect of our method: the possibility to determine, from interpolation, the correct a_k values corresponding to uncalibrated filter configurations. This is particularly important for limiting the number of calibrations necessary to achieve good prediction accuracy for any filter cascade. As simple case study, we predict the experimental filter penalties for the setup described in Fig.1, when the tunable optical filter is characterized by a 3 dB-bandwidth of 16.1GHz and 29.1GHz, respectively. To achieve this, we use calibrated a_k values for four filter configurations, at 14.8, 19.7, 25.2 and 31.5GHz (cf. Fig. 3). The order $N = 2$ of the extended SNR-OSNR relation described by Eq. (2) is selected to fit calibrated SNR_{dB}-$OSNR_{dB}$ curves, as a good trade-off between complexity and fitting accuracy (cf. Fig. 2). We interpolate a_k values corresponding to the 16.1 GHz and 29.1 GHz filters from the curves plotted in Fig. 3. For reference, we experimentally measure the SNR_{dB}-$OSNR_{dB}$ curves corresponding to the same filters and derive experimental $\underline{a_k}$ values as represented in Fig. 3. The deviation between measured and interpolated values does not exceed 2%.

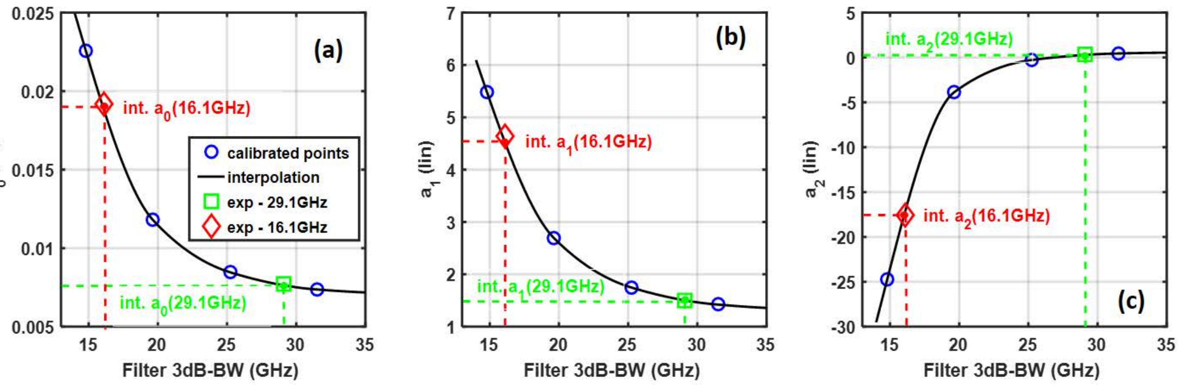

Figure 3: (a-c) Calibrated values of a_k coefficients (N = 2) based on four configurations of the tunable filter (steps 1-2) and interpolation (step 3) of a_k vs. filter 3 dB-bandwidth curves to determine a_k values corresponding to 3 dB-bandwidths of 16.1 GHz and 29.1 GHz, respectively.

In Fig. 4, we compare the predictions of filter penalties for both 19.1 GHz and 29.1GHz filters. In Fig. 4(a), we plot the experimental SNR_{dB}-$OSNR_{dB}$ curves (smoothed) obtained with and without optical filter. In Fig. 4(b), for comparison, we plot the filter SNR penalty ΔSNR, i.e. the vertical distance between the two curves plotted in Fig. 4(a), using three methods: directly from the experimental curves, from our interpolation method with $N = 2$ as described before, and finally, using the same interpolation method, but with a first-order SNR-OSNR relation

($N = 1$) as typically established in the literature [3,4]. Similarly, we plot in Fig. 4(c) the filter OSNR penalty ΔOSNR, i.e. the lateral distance between the two curves plotted in Fig.4(a).

In Fig. 4(b.1), it clearly appears that simply considering an additional order ($N = 2$) compared to [3,4] (i.e. $N = 1$) significantly reduces the prediction error on ΔSNR in case of strong filtering, from over 0.7 dB to less than 0.2 dB. As for the prediction error on ΔOSNR in Fig. 4(c.1), we observe similar gains in prediction accuracies. In case of moderate filtering however (BW=29.1GHz), considering N = 2 does not significantly improve penalty predictions compared to $N = 1$. It shows that for such filters, Φ as in $OSNR^{-1} = \Phi(SNR^{-1})$ is well described by a linear function.

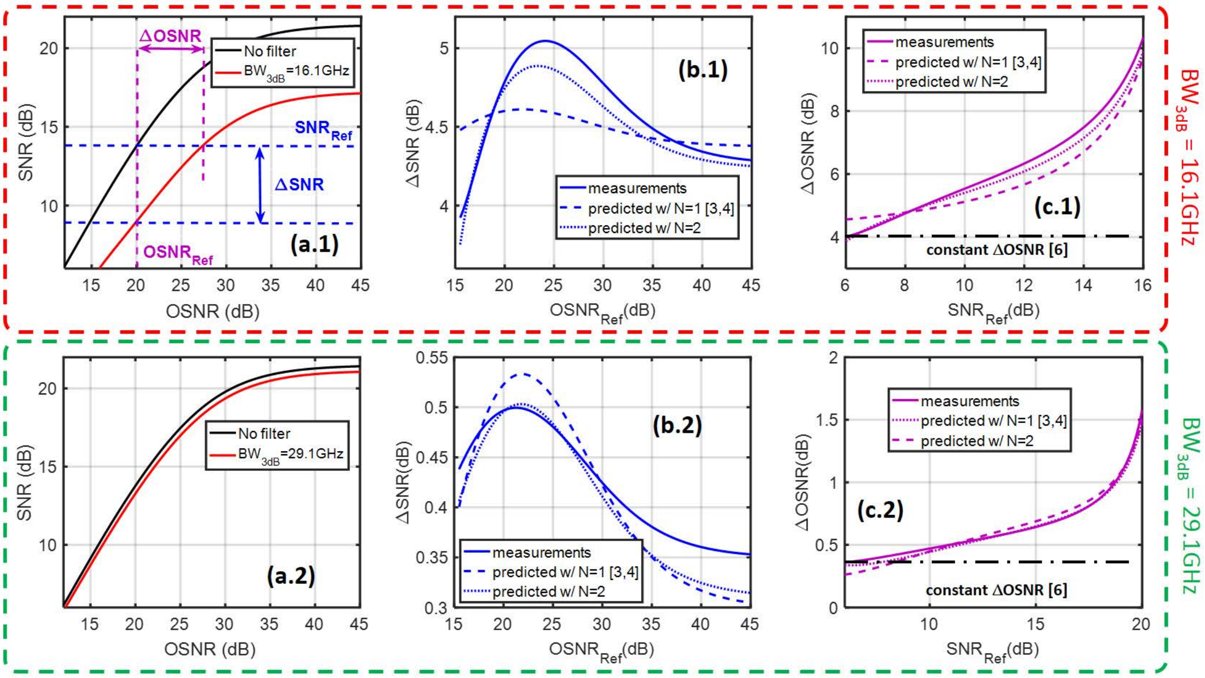

Figure 4: (a) SNR-OSNR curves with and without filter for calibrating filter penalty; (b) SNR filter penalty as function of the OSNR; and (c) OSNR penalty as function of the SNR.

Filtering penalties are typically counted as a constant OSNR penalty per filter [6]. In Fig. 4(c.2), we see that this method works well close to critical SNR levels for moderate filtering, and is thus adequate for current optical networks. For future dynamical optical networks with potentially stronger filtering impact and the need to evaluate margins whatever the SNR level, the method we propose shows much higher potential. Specifically, in Fig. 4(c.1), we show that our method can predict the OSNR penalty within 0.2 dB whatever the SNR, whereas a method predicting a constant OSNR penalty can underestimate it by up to 6dB for high SNR values.

5. CONCLUSIONS

We experimentally investigated the impact of tight optical filtering on SNR_{dB}-$OSNR_{dB}$ curves in back-to-back configuration. Compared to the literature, we showed it is more accurate to consider an extended SNR-OSNR relation accounting for equalization and its dependence on OSNR. We then proposed a generic, five-step method to evaluate the BER in presence of optical filtering. Under strong filtering, we showed the use of the extended SNR-OSNR relation within our method reduces SNR prediction errors from 0.7 dB to 0.2 dB. Whereas a constant OSNR penalty per filter is well-suited for current networks, we showed our method has much higher potential for future networks, with several dB gains on accuracy. Such performance predictions in presence of strong filtering will allow optical network design and optimization with reduced channel spacing and guard bands for an improved spectral efficiency. Alternatively, it will relax the specifications of WSS for low cost products.

ACKNOWLEDGEMENTS

This work was partly supported by H2020 EU project ORCHESTRA under grant agreement n°645360.

REFERENCES

[1] A. Carena *et al.*, *Journal of Lightwave Technology* **30**(10), 1524-1539 (2012)
[2] J. Proakis, "*Digital Communications*", McGraw-Hill, New York (1995)
[3] E. Torrengo *et al.*, *Optics Express* **19**(26), 790-798 (2011)
[4] F. Vacondio *et al.*, *Optics Express* **20**(2), 1022-1032 (2012)
[5] A. Stark *et al.*, *Journal of Lightwave Technology* **31**(21), 3352-3360 (2013)
[6] J. Pesic et al., in *Proc. OFC*, M3K.2 (2016)
[7] P. Jennevé *et al.*, in *Proc.* ACP, AS3E.2 (2015)